

Broadband Spectral Modelling of the Galactic Globular Cluster 47 Tucanae

Hambeleleni Davids,^{a,b,*} Christo Venter,^b Alice K Harding,^c Michael Backes^{a,b} and Anu Kundu^b

^a*Department of Physics, Chemistry & Material Science, University of Namibia, Windhoek Campus, Private Bag 13301, Windhoek, Namibia*

^b*Centre for Space Research, North-West University, Potchefstroom Campus, Private bag X6001, Potchefstroom 2520, South Africa*

^c*Theoretical Division, Los Alamos National Laboratory, Los Alamos, NM 87545, USA*
E-mail: hndiyavala@unam.na, christo.venter@nwu.ac.za, ahardingx@yahoo.com, mbackes@unam.na, anukundu02@yahoo.com

Terzan 5 is the only Galactic globular cluster that has plausibly been detected at very-high energies (VHEs; $E > 100$ GeV) by H.E.S.S., with 47 Tucanae (47 Tuc) being the densest and a very promising source in the Southern hemisphere for possible future detection in this band. 47 Tuc hosts the second-highest number of millisecond pulsars (29 detected in the radio so far). We model the broadband spectral energy distribution of this cluster, attributing this to cumulative pulsed emission from a population of embedded millisecond pulsars, as well as unpulsed emission from the interaction of their leptonic winds with the ambient magnetic and soft-photon fields. Our model invokes an unpulsed inverse Compton (IC) component to model the TeV data and cumulative pulsed curvature radiation to fit the GeV *Fermi* data, and it explains the *Chandra* X-ray spectrum via a pulsed synchrotron radiation (SR) component from electron-positron pairs originating from within the pulsar magnetospheres. An unpulsed SR component can explain the radio data. Using our model, we constrain model parameters and start breaking degeneracies among them. We lastly present predictions of the spectral shape of 47 Tuc as it would appear to CTA.

High Energy Astrophysics in Southern Africa 2022 - HEASA2022
28 September - 1 October 2022
Brandfort, South Africa

*Speaker

1. The Galactic Globular Cluster 47 Tucanae (47 Tuc)

Globular clusters (GCs) are ancient, gravitationally bound stellar systems consisting of 10^4 – 10^6 stars, with ages ranging between 11 and 13 Gyr [1–3]. About 160 GCs have been detected in the Milky Way with radio and/or optical detectors [4]. 47 Tuc is a massive GC ($M \sim 10^6 M_\odot$, [5]) within our Galaxy and it is best known for its richness in exotic stellar populations, i.e., there are 300 known X-ray sources including 19 known binary pulsars, five quiescent, low-mass X-ray binaries (LMXBs) containing accreting neutron stars, and one stellar black hole candidate [6, 7].

47 Tuc is a nearby GC, located at 4.5 kpc. Interestingly, 29 radio millisecond pulsars (MSPs) have been identified in this GC, and the total number is estimated to be much more than 30 [6, 8, 9]. This means that 47 Tuc hosts the second highest number of detected MSPs in any GC, after Terzan 5¹. This source is a favourite observational target, although its stellar population is computationally quite challenging to model because of the large number of stars and its high central density [10].

GCs are multi-wavelength objects visible in the radio to γ -ray band. Within the MSP scenario [11], the emission components of these objects are thought to emanate from cumulative magnetospheric and diffuse emission by particles accelerated either within the pulsar magnetospheres or in interstellar shocks. Several observations of 47 Tuc have been carried out so far. Radio observations have been conducted, with no statistically significant evidence for radio emission from the central region for the cluster. However, the cluster showed a 2.5σ signal near the centre that may be confirmed by future deeper radio observations [12]. Diffuse X-ray emission was detected [13] and a reasonable description of the observed profile was obtained. 47 Tuc was first detected in γ -rays by the *Fermi* Large Area Telescope (LAT; [14, 15]) with the spectral energy distribution (SED) similar to that of MSPs [8, 14, 16]. Observations of 47 Tuc were also performed with H.E.S.S., leading to an upper limit on the integral γ -ray flux of $F(E > 800 \text{ GeV}) < 6.7 \times 10^{-13} \text{ cm}^{-2} \text{ s}^{-1}$ [17].

2. The Multi-wavelength Observations of 47 Tuc

2.1 Diffuse X-ray emission

There has been a search for diffuse X-ray emission by [18] from the core regions of 10 GCs using *Chandra* data, allowing unresolved X-ray emission to be found for four clusters. The X-ray emission is understood to be due to unresolved faint point source populations in the cores of the clusters. Another group also searched for diffuse X-ray emission from GCs, however, they excluded 47 Tuc from their target list [19]. They detected diffuse X-ray emission associated with Terzan 5 outside its half-mass radius and found that the emission spectrum can be characterised by a power law (PL).

In addition to this, [13] also searched for diffuse X-ray emission in 47 Tuc and found a detection in the region from twice the core radius, $2r_c$, up to $\sim 4'$ from the centre of the cluster. They fitted the spectrum using an absorbed PL model and a thermal plasma model, but did not find a good fit with these. However, when they added a thermal component to the PL model, they obtained a reasonable description of the observed spectrum. To quantify the distribution of the X-ray emission with angular distance from the cluster centre, the researchers divided the region of interest (RoI)

¹<http://www.naic.edu/~pfreire/GCpsr.html>

into five rings. The surface brightness profile was obtained by integrating the best-fit models for each ring over the full energy band 0.5 – 7.0 keV. The total surface brightness showed an exponential decay. The spatial distribution of non-thermal X-ray flux also follows an exponential decay that conforms with the stellar density profile of 47 Tuc, while the plasma or non-thermal component seems to be uniform. This aligns with the idea that if there are many stars and MSPs at the centre of the cluster, one would expect brighter emission there, with the surface brightness decreasing outward as the stellar density drops.

2.2 High-Energy gamma-ray emission

GCs are expected to emit γ -rays because they have a large population of MSPs, since these are efficient particle accelerators and because many individual MSPs emit pulsed γ -ray emission. *Fermi* reported the detection of γ -ray emissions above 200 MeV at a significance level of 17σ from 47 Tuc and noted that the observed γ -ray luminosity implies an upper limit of 60 MSPs present in 47 Tuc [14]. Prior to 47 Tuc being detected by *Fermi*, a pulsar model was applied that invoked a Monte-Carlo method and took different inclination and observer angles into account, predicting the cumulative curvature radiation (CR) spectrum for 100 pulsars. They predicted the GeV spectrum of 47 Tuc within a factor of 2 of the eventual detection, in both energy and flux level [20].

2.3 VHE gamma-ray observations

H.E.S.S. searched for VHE γ -ray sources associated with selected GCs, including 47 Tuc, aiming to put constraints on leptonic emission models. They searched for both point-like and extended VHE γ -ray emission from their sample and also performed a stacking analysis, combining the data from all selected GCs. They calculated the expected γ -ray flux from each of the selected GCs, based on their number of host MSPs, their optical brightness, and the energy density of background photon fields. No VHE γ -ray emission was significantly detected from any of the selected GCs, including 47 Tuc. However, [21] noted that H.E.S.S. may detect 47 Tuc provided they observe this cluster for at least 100 hours.

3. Previous GC models

There are several models that predict the multi-wavelength spectrum radiated by GCs. For example, [22] studied a scenario where leptons are accelerated by MSPs in relativistic, interstellar shocks that are created when their winds collide with each other inside the cores of clusters. These leptons are thought to upscatter ambient photons via IC scattering, which may lead to unpulsed GeV to TeV spectral emission components. They calculated the GeV–TeV γ -ray spectra for different models of injection of leptons and parameters of the GCs and showed results for four specific GCs, including 47 Tuc. They argued that the best candidates that might be detected by the Cherenkov telescopes are 47 Tuc in the Southern hemisphere and M13 in the Northern hemisphere.

Furthermore, some researchers modelled the cumulative pulsed GeV flux via CR from MSP magnetospheres by assuming a pair-starved polar cap E -field [23]. The cumulative pulsed CR from 100 pulsars was modelled by [20], where they randomized the MSP geometry, as well as period and period time derivative. [20] later refined their approach and predicted the GeV spectrum of 47 Tuc.

On the other hand, [24] considered an alternative scenario to produce GeV emission and calculated unpulsed IC radiation from electrons and positrons upscattering the cosmic microwave background (CMB), stellar photons, and the Galactic background. This is in contrast to the usual assumption that the GeV emission measured by *Fermi* is due to pulsed CR. They showed that the γ -ray spectrum from 47 Tuc can be explained by upward scattering of either the relic photons, the Galactic infrared photons, or the Galactic stellar photons.

Finally, [25] explored a model based on γ -ray burst (GRB) remnants as sources of energetic leptons and hadrons. When one considers a short burst that is caused by two merging NSs, some fraction of the shock wave energy might be tapped to accelerate hadrons following the explosion. [25] constrained the spatial diffusion coefficient κ_0 using the observed VHE extension of HESS J1747–248 (the γ -ray source associated with Terzan 5). They then compared the burst age with the short burst occurrence rate and concluded that the detected source extension is compatible with a relatively slow diffusion of hadrons in the GC. [25] also noted that there might be many multi-wavelength signatures that may provide support for this scenario, for example, diffuse thermal X-rays arising from hot plasma, and diffuse X-rays from IC by electrons accelerated by the blast wave.

4. Our spectral models

4.1 The GC leptonic model – unpulsed emission

We fit multi-wavelength data of 47 Tuc using the model of [11] that calculates the particle transport (including diffusion and radiation losses) in a spherically symmetric, stationary approach. The model assumes that the MSPs are at the very centre of the cluster and they inject particles that diffuse throughout the cluster; as a result, unpulsed low-energy SR (LESR) and unpulsed IC components are produced. The main free parameters incorporated in the model are: cluster magnetic field (B), power-law index (Γ) of the injected particle spectrum (the particles are assumed to have undergone acceleration in inter-pulsar shocks), number of stars in the cluster (N), distance to the cluster (d), the average spin-down luminosity per pulsar ($\langle \dot{E} \rangle$), the conversion efficiency of spin-down luminosity into particle acceleration (η), and number of MSPs in the GC (N_{MSP}).

4.2 The leptonic pulsar model – cumulative pulsed emission

We also use a model of pulsed high-energy radiation over the entire electromagnetic spectrum, from optical to VHE γ -ray wavelengths [26]. In this model, the authors assumed that primary electrons radiate pulsed CR and electron-positron pairs radiate SR. The primary particles are accelerated by an electric field induced by rotation of the magnetic field, while the pairs originate in polar cap (PC) cascades that are initiated in the strong B -fields near the NS surface. [27] showed a schematic of this model, applied to the Vela pulsar. The accelerated primary particles travel along the separatrix that separates the open and closed B -field lines and extend into the current sheet, while for the secondary particles, there is a PC cascade producing electron-positron pairs at low altitudes. These pairs radiate SR at high altitude that makes up the high-energy SR (HESR) component.

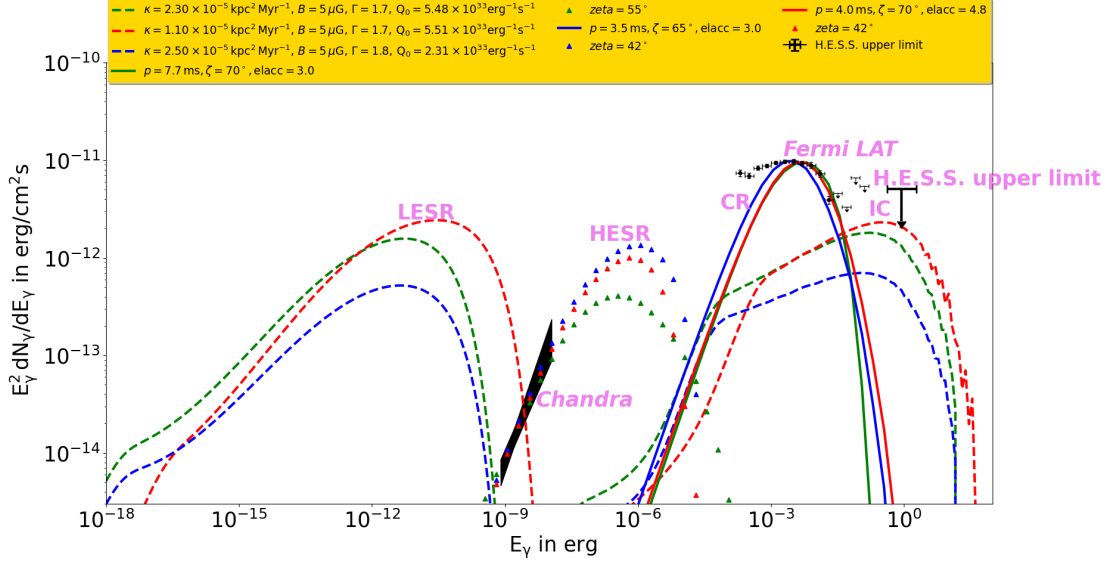


Figure 1: Spectral components for 47 Tuc predicted using the leptonic models of [11] and [26]. For the LESR and IC components (dashed lines), we used the following parameters: diffusion coefficient $\kappa = 2.30 \times 10^{-5} \text{ kpc}^2 \text{ Myr}^{-1}$, $B = 5 \mu\text{G}$, $\Gamma = 1.7$, $Q_0 = 5.48 \times 10^{33} \text{ erg}^{-1} \text{ s}^{-1}$ for the green lines, $\kappa = 1.10 \times 10^{-5} \text{ kpc}^2 \text{ Myr}^{-1}$, $B = 5 \mu\text{G}$, $\Gamma = 1.7$, $Q_0 = 5.51 \times 10^{33} \text{ erg}^{-1} \text{ s}^{-1}$ for the red lines, and $\kappa = 2.50 \times 10^{-5} \text{ kpc}^2 \text{ Myr}^{-1}$, $B = 5 \mu\text{G}$, $\Gamma = 1.8$, $Q_0 = 2.31 \times 10^{33} \text{ erg}^{-1} \text{ s}^{-1}$ for the blue lines. The HESR (triangles) and CR (solid lines) components are predictions using the model of [26] for the parameters period $P = 7.7 \text{ ms}$, observer angle $\zeta = 70^\circ$, acceleration rate $R_{\text{acc}} = eE_{\parallel}/m_e c^2 = 3.0 \text{ cm}^{-1}$, $N_{\text{MSP}} = 40$ (green CR component), $\zeta = 55^\circ$, $N_{\text{MSP}} = 65$ (green SR component), $P = 3.5 \text{ ms}$, $\zeta = 65^\circ$, $R_{\text{acc}} = 3.0$, $N_{\text{MSP}} = 40$ (blue CR component), $\zeta = 42^\circ$, $N_{\text{MSP}} = 40$ (blue SR component), $P = 4.0 \text{ ms}$, $\zeta = 70^\circ$, $R_{\text{acc}} = 4.8$, $N_{\text{MSP}} = 45$ (red CR component), and $\zeta = 42^\circ$, $N_{\text{MSP}} = 29$ (red SR component). We have assumed a pair multiplicity of 3.0×10^3 for all SR components. We also indicate *Chandra* [13] and *Fermi* LAT data [29], and the H.E.S.S. [30] upper limit.

5. Broadband SED of 47 Tuc

We present spectral fits to the SED of 47 Tuc using the pulsed and unpulsed models described above. Here we fit the *Chandra* data using the HESR component and the *Fermi* data using the cumulative primary CR component of pulsed γ -ray emission originating in the magnetospheres of MSPs embedded in the GC. We also model the unpulsed IC component, such that it is consistent with the H.E.S.S. upper limits. Several model parameters are used to obtain reasonable fits for the data, with our best fit being the red components (see Figure 1). Looking at the fit of the *Fermi* data, the model does not fit the data very well. That is, the CR component is not broad enough to fit the data. We therefore think that we could improve our fit by using the synchro-curvature model presented by [28] and first applied to Vela. This will be the subject of a future paper.

6. MSP population energetics

Even though our model provides reasonable fits to the X-ray and high-energy data, one still needs to consider whether *Chandra* has detected the “unresolved MSPs” postulated by the model

Table 1: Sample parameter combinations that lead to a balance of the X-ray energetics. The units of the spin-down powers are erg s^{-1} , and α denotes the index of the PL function $dN/d\dot{E}$.

η^X	$\langle \dot{E} \rangle_{\text{invis}}$	$\langle \dot{E} \rangle_{\text{vis}}$	\dot{E}_{min}	\dot{E}_{max}	α	N_{vis}^X	N_{invis}^X	N_{tot}^X
0.02%	1.3×10^{32}	4.6×10^{34}	10^{29}	2.4×10^{35}	0.21	27	394	421
0.21%	9.7×10^{31}	2.9×10^{33}	9.0×10^{30}	10^{34}	0.03	39	49	88
0.35%	3.3×10^{31}	1.6×10^{33}	1.1×10^{29}	5.0×10^{33}	-0.04	43	85	128
0.5%	1.3×10^{31}	2.2×10^{33}	4.3×10^{29}	1.6×10^{34}	0.31	21	149	170
1%	4.3×10^{31}	5.6×10^{32}	2.1×10^{31}	2.1×10^{33}	0.13	42	23	65
1%	4.1×10^{31}	9.6×10^{32}	2.1×10^{31}	1.1×10^{34}	0.48	25	24	49
1%	5.6×10^{31}	1.2×10^{33}	4.0×10^{31}	2×10^{37}	0.96	19	18	37

to explain the diffuse X-ray flux seen by [13], i.e., can one explain the observed SR flux for a reasonable number of resolved and unresolved MSPs? We want to know if the given number of MSPs is adequate to emit the cluster luminosity measured in the X-ray band. Therefore, we should consider the population properties and emission energetics of the MSPs.

Let us consider total of N_{MSPs} pulsars, having an average spin-down luminosity $\langle \dot{E} \rangle$. The X-ray luminosity is produced by N_{vis}^X pulsars that convert their spin-down luminosity into X-rays with an efficiency η_{vis}^X :

$$L_{\text{X,vis}} = \eta_{\text{vis}}^X N_{\text{vis}}^X \langle \dot{E} \rangle. \quad (1)$$

Similarly, the diffuse emission is produced by N_{invis}^X unresolved pulsars:

$$L_{\text{X,invis}} = \eta_{\text{invis}}^X N_{\text{invis}}^X \langle \dot{E} \rangle. \quad (2)$$

Let us assume that the pulsar spin-down powers are distributed according to some distribution function $dN/d\dot{E}$. We can then recover the total number of MSPs, total number of MSPs detectable in the X-ray band, and total number of undetected MSPs in the X-ray band.

$$N_{\text{tot}}^X = \int_{\dot{E}_{\text{min}}}^{\dot{E}_{\text{max}}} \left(\frac{dN}{d\dot{E}} \right) d\dot{E}, \quad (3)$$

$$N_{\text{det}}^X = \int_{\dot{E}_{\text{b}}}^{\dot{E}_{\text{max}}} \left(\frac{dN}{d\dot{E}} \right) d\dot{E}, \quad (4)$$

$$N_{\text{undet}}^X = \int_{\dot{E}_{\text{min}}}^{\dot{E}_{\text{b}}} \left(\frac{dN}{d\dot{E}} \right) d\dot{E}. \quad (5)$$

Lastly, we can derive the average spin-down power for the group of detectable vs. undetectable pulsars by defining a break spin-down power \dot{E}_{b} , as well as minimum and maximum powers \dot{E}_{min} and \dot{E}_{max} :

$$\langle \dot{E} \rangle_{\text{det}} = \frac{1}{N_{\text{det}}^X} \int_{\dot{E}_{\text{b}}}^{\dot{E}_{\text{max}}} \dot{E} \left(\frac{dN}{d\dot{E}} \right) d\dot{E}, \quad (6)$$

$$\langle \dot{E} \rangle_{\text{undet}} = \frac{1}{N_{\text{undet}}^X} \int_{\dot{E}_{\text{min}}}^{\dot{E}_{\text{b}}} \dot{E} \left(\frac{dN}{d\dot{E}} \right) d\dot{E}. \quad (7)$$

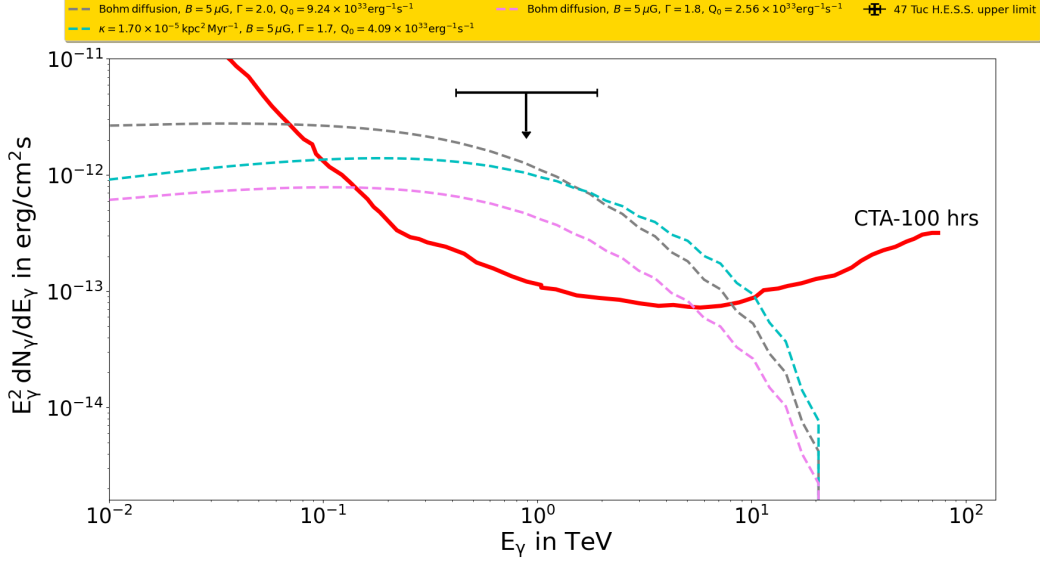


Figure 2: CTA predictions of 47 Tuc spectra. For the example spectra, we assume Bohm diffusion, $B = 5 \mu\text{G}$, $\Gamma = 2.0$, $Q_0 = 9.24 \times 10^{33} \text{erg}^{-1} \text{s}^{-1}$ for the gray dashed line, $\kappa = 1.70 \times 10^{-5} \text{kpc}^2 \text{Myr}^{-1}$, $B = 5 \mu\text{G}$, $\Gamma = 1.7$, $Q_0 = 4.09 \times 10^{33} \text{erg}^{-1} \text{s}^{-1}$ for the cyan dashed line, and Bohm diffusion, $B = 5 \mu\text{G}$, $\Gamma = 1.8$, $Q_0 = 2.56 \times 10^{33} \text{erg}^{-1} \text{s}^{-1}$ for the magenta dashed line. The H.E.S.S. upper limit [30] is indicated by the black arrow and the CTA sensitivity [31] for 100 hours of observations time as a red solid line.

Since we do not know the distribution of pulsar spin-down power, we postulate that it might follow a PL. We can then see if there are reasonable parameter combinations that yield the correct X-ray luminosity (see Table 1 for typical parameter solutions that satisfy the X-ray luminosity constraints). In future, one may consider a different distribution function, including a broken power law, to constrain the energetics of the embedded MSP population.

7. Future observations by the Cherenkov Telescope Array (CTA)

Regarding future VHE observations of 47 Tuc, the Cherenkov Telescope Array (CTA) has a better chance of detecting this cluster and possibly measuring the spectrum quite well, which will constrain the cluster’s VHE spectral shape. Figure 2 shows different predicted spectral shapes of 47 Tuc. In the near future, CTA should be able to discriminate between these shapes, which will allow us to constrain model parameters more robustly. The CTA should also reveal more GCs in the VHE band, adding to the list of VHE GCs that presently contain only a single member (Terzan 5).

8. Conclusion

There are several models that attempted to explain the broadband emission from 47 Tuc. In this paper, we used both the unpulsed and pulsed codes to fit the multi-wavelength data of 47 Tuc. We find reasonable fits to its SED, but the CR component is not broad enough to fit the high-energy data. We will therefore update our modelling in future, using a synchro-curvature component that may yield a broader spectral peak (Davids et al., in prep.). We have also presented different

predictions of the IC spectral shape of 47 Tuc. Future observations by CTA will (hopefully) allow us to better constrain our parameters. Lastly, we derived degenerate but plausible constraints on the energetics of the MSP population embedded in 47 Tuc. Continued multi-wavelength observations should allow us to better constrain our model parameters, break degeneracies between parameters, improve our models, and perhaps even discriminate between competing models.

Acknowledgments

This work is based on the research supported wholly / in part by the National Research Foundation of South Africa (NRF; Grant Numbers 87613, 90822, 92860, 93278, 99072, and 132264). The Grant holder acknowledges that opinions, findings and conclusions or recommendations expressed in any publication generated by the NRF supported research are that of the author(s), and that the NRF accepts no liability whatsoever in this regard. The Virtual Institute for Scientific Computing and Artificial Intelligence (VI-SCAI) is gratefully acknowledged for operating the High Performance Computing (HPC) cluster at the University of Namibia (UNAM). VI-SCAI is partly funded through a UNAM internal research grant. This study was financially supported by SA-GAMMA.

References

- [1] L.M. Krauss and B. Chaboyer, *Age Estimates of Globular Clusters in the Milky Way: Constraints on Cosmology*, *Science* **299** (2003) 65.
- [2] A. Marín-Franch et al., *The ACS Survey of Galactic Globular Clusters. VII. Relative Ages*, *ApJ* **694** (2009) 1498 [0812.4541].
- [3] D.A. Forbes and T. Bridges, *Accreted versus in situ Milky Way globular clusters*, *MNRAS* **404** (2010) 1203 [1001.4289].
- [4] W.E. Harris, *A Catalog of Parameters for Globular Clusters in the Milky Way*, *AJ* **112** (1996) 1487.
- [5] C. Pryor and G. Meylan, *Velocity Dispersions for Galactic Globular Clusters*, in *Structure and Dynamics of Globular Clusters*, S.G. Djorgovski and G. Meylan, eds., vol. 50 of *Astronomical Society of the Pacific Conference Series*, p. 357, Jan., 1993.
- [6] C.O. Heinke et al., *A Deep Chandra Survey of the Globular Cluster 47 Tucanae: Catalog of Point Sources*, *ApJ* **625** (2005) 796 [astro-ph/0503132].
- [7] J.C.A. Miller-Jones, J. Strader, C.O. Heinke, T.J. Maccarone, M. van den Berg, C. Knigge et al., *Deep radio imaging of 47 Tuc identifies the peculiar X-ray source X9 as a new black hole candidate*, *MNRAS* **453** (2015) 3918 [1509.02579].
- [8] J.E. Grindlay, C. Heinke, P.D. Edmonds and S.S. Murray, *High-Resolution X-ray Imaging of a Globular Cluster Core: Compact Binaries in 47Tuc*, *Science* **292** (2001) 2290 [astro-ph/0105528].

- [9] A.A. Abdo et al., *A population of gamma-ray emitting globular clusters seen with the Fermi Large Area Telescope*, *A&A* **524** (2010) A75.
- [10] C.S. Ye, K. Kremer, C.L. Rodriguez, N.Z. Rui, N.C. Weatherford, S. Chatterjee et al., *Compact Object Modeling in the Globular Cluster 47 Tucanae*, *ApJ* **931** (2022) 84 [2110.05495].
- [11] A. Kopp, C. Venter, I. Büsching and O.C. De Jager, *Multi-wavelength Modeling of Globular Clusters—The Millisecond Pulsar Scenario*, *ApJ* **779** (2013) 126.
- [12] T.-N. Lu and A.K.H. Kong, *Radio Continuum Observations of 47 Tucanae and ω Centauri: Hints for Intermediate-mass Black Holes?*, *ApJ* **729** (2011) L25 [1102.1668].
- [13] E.M.H. Wu et al., *Chandra Detection of a New Diffuse X-Ray Component from the Globular Cluster 47 Tucanae*, *ApJL* **788** (2014) L40.
- [14] A.A. Abdo et al., *Detection of High-Energy Gamma-Ray Emission from the Globular Cluster 47 Tucanae with Fermi*, *Science* **325** (2009) 845.
- [15] W.B. Atwood, A.A. Abdo, M. Ackermann, W. Althouse, B. Anderson, M. Axelsson et al., *The Large Area Telescope on the Fermi Gamma-Ray Space Telescope Mission*, *ApJ* **697** (2009) 1071 [0902.1089].
- [16] P.C.C. Freire et al., *Fermi Detection of a Luminous γ -Ray Pulsar in a Globular Cluster*, *Science* **334** (2011) 1107 [1111.3754].
- [17] F. Aharonian et al., *HESS upper limit on the very high energy γ -ray emission from the globular cluster 47 Tucanae*, *A&A* **499** (2009) 273 [0904.0361].
- [18] C.Y. Hui, K.S. Cheng and R.E. Taam, *Diffuse X-ray Emission in Globular Cluster Cores*, *ApJ* **700** (2009) 1233 [0905.2908].
- [19] P. Eger, W. Domainko and A.-C. Clapson, *Chandra detection of diffuse X-ray emission from the globular cluster Terzan 5*, *A&A* **513** (2010) A66 [1002.0711].
- [20] C. Venter and O.C. de Jager, *Constraining A General-Relativistic Frame-Dragging Model for Pulsed Radiation from a Population of Millisecond Pulsars in 47 Tucanae using GLAST LAT*, *ApJ* **680** (2008) L125 [0805.1809].
- [21] H. Ndiyavala, P.P. Krüger and C. Venter, *Identifying the brightest Galactic globular clusters for future observations by H.E.S.S. and CTA*, *MNRAS* **473** (2018) 897 [1708.09817].
- [22] W. Bednarek and J. Sitarek, *High-energy γ -rays from globular clusters*, *MNRAS* **377** (2007) 920.
- [23] A.K. Harding, V.V. Usov and A.G. Muslimov, *High-Energy Emission from Millisecond Pulsars*, *ApJ* **622** (2005) 531 [astro-ph/0411805].

- [24] K.S. Cheng, D.O. Chernyshov, V.A. Dogiel, C.Y. Hui and A.K.H. Kong, *The Origin of Gamma Rays from Globular Clusters*, *ApJ* **723** (2010) 1219 [1009.2278].
- [25] W.F. Domainko, *Finding short GRB remnants in globular clusters: the VHE gamma-ray source in Terzan 5*, *A&A* **533** (2011) L5 [1106.4397].
- [26] A.K. Harding and C. Kalapotharakos, *Synchrotron Self-Compton Emission from the Crab and Other Pulsars*, *ApJ* **811** (2015) 63 [1508.06251].
- [27] A.K. Harding, C. Kalapotharakos, M. Barnard and C. Venter, *Multi-TeV Emission from the Vela Pulsar*, *ApJ* **869** (2018) L18 [1811.11157].
- [28] A.K. Harding, C. Venter and C. Kalapotharakos, *Very-high-energy Emission from Pulsars*, *ApJ* **923** (2021) 194 [2110.09412].
- [29] A.M. Brown, T. Lacroix, S. Lloyd, C. Boehm and P. Chadwick, *Understanding the γ -ray emission from the globular cluster 47 Tuc: Evidence for dark matter?*, *PhRvD* **98** (2018) 041301 [1806.01866].
- [30] A. Abramowski et al., *Search for very-high-energy γ -ray emission from Galactic globular clusters with H.E.S.S.*, *A&A* **551** (2013) A26.
- [31] S. Funk, J.A. Hinton and CTA Consortium, *Comparison of Fermi-LAT and CTA in the region between 10-100 GeV*, *Astropart. Phys.* **43** (2013) 348 [1205.0832].